



HAL
open science

Damage mechanisms characterization of flax fibers–reinforced composites with interleaved natural viscoelastic layer using acoustic emission analysis

Abderrahim El Mahi, Hajer Daoud, Jean-Luc Rebiere, Isabelle Gimenez,
Mohamed Taktak, Mohamed Haddar

► **To cite this version:**

Abderrahim El Mahi, Hajer Daoud, Jean-Luc Rebiere, Isabelle Gimenez, Mohamed Taktak, et al.. Damage mechanisms characterization of flax fibers–reinforced composites with interleaved natural viscoelastic layer using acoustic emission analysis. *Journal of Composite Materials*, 2019, 53 (18), pp.2623-2637. 10.1177/0021998319836236 . hal-02954704

HAL Id: hal-02954704

<https://hal.science/hal-02954704>

Submitted on 14 Mar 2024

HAL is a multi-disciplinary open access archive for the deposit and dissemination of scientific research documents, whether they are published or not. The documents may come from teaching and research institutions in France or abroad, or from public or private research centers.

L'archive ouverte pluridisciplinaire **HAL**, est destinée au dépôt et à la diffusion de documents scientifiques de niveau recherche, publiés ou non, émanant des établissements d'enseignement et de recherche français ou étrangers, des laboratoires publics ou privés.

Damage mechanisms characterization of flax fibers–reinforced composites with interleaved natural viscoelastic layer using acoustic emission analysis

Abderrahim El Mahi¹, Hajer Daoud^{1,2}, Jean-Luc Rebiere¹, Isabelle Gimenez³, Mohamed Taktak² and Mohamed Haddar²

Abstract

In this paper, the static and fatigue behavior of flax fiber-reinforced composites with and without an interleaved natural viscoelastic layer are investigated. Viscoelastic composite plates consist of a soft natural viscoelastic layer which is confined between two identical flax fiber reinforced composites. Different stacking sequences of specimens are tested with uniaxial tensile loading until failure. The mechanical behavior and the acoustic activity of damage sources in various configurations with and without a viscoelastic layer are compared. The analysis of acoustic emission signals and the macroscopic and microscopic observations led to the identification of the main acoustic signatures of different damage modes dominant in each type of composites (with and without a viscoelastic layer). These results allow better identification of the influence of the impact of a viscoelastic layer on the mechanical behavior of different composites. In addition, static and fatigue flexural behavior of unidirectional composites with and without viscoelastic layer are characterized in 3-point bending tests. The effects of viscoelastic layer on the stiffness, hysteresis loops, and loss factor are studied for various numbers of cycles during cyclic fatigue.

Keywords

Composite, flax fibers, natural viscoelastic layer, tensile, flexural, fatigue, damage

Introduction

Composite materials have been increasingly used in various types of engineering systems such as aeronautics, aerospace, civil engineering, sport, and leisure industries to minimize structural weight. Interest in environmental and ecological concerns in recent years has driven the development of bio-based composites with high mechanical performance. Vegetable fibers are proving to be much more interesting and can sometimes even compete with certain synthetic fibers, such as glass fibers.¹ For this reason, numerous studies have been carried out on reinforced composites of various vegetable fibers,² in particular, studies on flax fibers,^{3–5} hemp,⁶ or sisal fibers,⁷ which are well known for their good mechanical properties. They demonstrate that bio-based composites present many advantages such as their low density, biodegradability, and their relatively high specific mechanical properties.

A viscoelastic layer has a level of energy dissipation; therefore it plays an important role in damping and improves the dynamic response of the structure. In any practical dynamic design, damping is an important aspect as it significantly impacts vibration propagation. A viscoelastic laminated composite plate consists of a soft viscoelastic core which is confined between two identical elastic surface layers. This is a type of constraining damping where the structure uses the damping properties of the viscoelastic layer by inducing

¹Acoustics Laboratory of Le Mans University (LAUM), France

²Laboratory of Mechanics Modeling and Production (LA2MP), National School of Engineers of Sfax, University of Sfax, Tunisia

³Centre de Transfert de Technologie du Mans, France

Corresponding author:

Hajer Daoud, Ecole Nationale d'Ingenieurs de Sfax Route de Soukra Km 4 Sfax, 3038 Tunisia.

Email: daoud.hajer@yahoo.fr

high shear strain in the material on out-of-plane motion.⁸ Thus, it appears that the combination of laminate tailoring with interlaminar viscoelastic layers will offer the advantages of high damping associated with good mechanical properties and low weight. Moreover, the interlaminar damping concept is highly compatible with the production processes of laminated structures. Bhimaraddi⁹ has studied the analysis of sandwich beams and constrained layer damping in beams. The sandwich beam theory has been used to determine the loss factors of a viscoelastically damped beam. Khalfi and Ross¹⁰ have investigated the effect of inserting a viscoelastic layer on the transient response of a plate. An analytical model of a plate with partial constrained layer damping has been used to obtain the harmonic and transient responses due to an impact. Several other studies on the theoretical and experimental behavior of composites with viscoelastic layers have been reported in the literature.^{11–14} Modeling the mechanical behavior of composite laminates with interlaminar layers was developed by Saravanos and Pereira¹¹ using a discrete-layer laminate theory. A first-order shear deformation theory is used by Cupial and Niziol¹² to evaluate dynamic properties of a rectangular three-layered plate with a viscoelastic core layer and laminated faces.

The acoustic emission (AE) technique has been often used for the identification and characterization of micro failure mechanisms in composites.^{15,16} Microstructural changes in materials release strain energy, resulting in the propagation of acoustic waves. These signals are recorded by sensors fixed on the material. Then, features are deduced from these acoustic bursts. Among them, temporal features are often used, such as amplitudes, energies, rise times, etc.^{17–19} Moreover, AE works performed on glass or carbon fiber reinforced composites often involve mixed time–frequency analyses.^{19–23} The AE technique has also been used for several natural fiber composites with different reinforcements and matrices^{24–27} and at different observation scales. Several phenomena can be distinguished, such as matrix cracking and matrix/matrix friction.^{19,28} At the composite scale, amplitudes between 40 dB and 60 dB are usually attributed to matrix cracking. Fiber/matrix debonding is often attributed to amplitudes between 45 dB and 70 dB. Of course, the values of these intervals depend on the kind of fibers and matrix used. Friction phenomena (matrix/matrix or matrix/fiber) are sometimes ignored or included in the previous categories. Aslan²⁹ distinguished these events in the case of flax/low-melting-temperature polyethylene terephthalate (LPET) composites. Fiber failures are attributed to the events exhibiting the highest amplitudes and energies. In particular cases, especially for crossed ply composites, the AE technique can be used

to detect delamination.³⁰ However, this global phenomenon contains several damage mechanisms such as fiber pullout and cracking, or fiber/matrix friction. Despite an increasing number of multi-parametric studies, it is worth emphasizing that amplitude remains the classification feature most often discussed in the literature for natural fiber composites. Data concerning features such as duration and energy are less common.^{28,29}

Very few studies on bio-composites have looked at inserting a natural viscoelastic layer. The objective of this research is to analyze the static and fatigue behavior of flax fiber reinforced composites with and without an interleaved natural viscoelastic layer.

Different stacking sequences of specimens were tested with uniaxial tensile and flexural loading until failure. Moreover, the tensile tests were monitored by AE techniques. The main objective was to identify the failure mechanisms occurring under load, and to correlate their effects with the tensile behavior of the material. Thus, the results obtained from the analysis of AE signals associated to those of the macroscopic and microscopic observations will lead to the identification of the main acoustic signatures of different damage modes dominant in each type of composites.

Materials and experimental setup

Materials

The materials considered in the analysis are elastic and viscoelastic laminate materials. A viscoelastic laminate material consists of a soft natural viscoelastic layer of natural rubber which is confined between two identical elastic laminates. The mechanical characteristics of this layer are presented in Table 1.

The composite materials were made up of unidirectional long flax fibers manufactured by LINEO³¹ in partially bio-based epoxy resin (green epoxy resin 56) manufactured by SICOMIN. The weights of unidirectional long flax fibers were 200 g⁻². The laminate materials were prepared by a hand layup process from epoxy resin with hardener, flax fibers, and a natural viscoelastic layer. Plates of different dimensions were cured at room temperature under pressure using a vacuum molding process, and then post-cured in an oven. The plates were fabricated with 8 or 16 layers in such a way as to obtain a total thickness of 4 or 8 mm for laminates

Table 1. The mechanical characteristics of the viscoelastic layer.

	<i>E</i> (MPa)	Density (Kg/m ³)	Hardness (shore A)
Viscoelastic layer	2	950	40

and 5 and 9 mm for viscoelastic laminates (on the z axis) with the same reinforcement volume fraction (between 38% and 45% for all the specimens). The middle plane (xy plane) of the laminate was a symmetrical plane. The void content of the material was calculated by comparing the measured density of the composite to its theoretical density calculated from the volume fraction of fiber and matrix. The void fraction of the material was determined to be between 10% and 15%.

The engineering constants for the orthotropic material were measured using tensile tests on unidirectional specimens having different orientations of the unidirectional plies at 0° , 45° , and 90° . The values obtained are shown in Table 2. For the tensile tests, three types of unidirectional specimens were prepared, with fiber directions of 90° , 45° , and 0° . They were labeled $[90]_8$, $[45]_8$, and $[0]_8$ without a viscoelastic layer and $[90_4/V]_s$, $[45_4/V]_s$, and $[0_4/V]_s$ with a natural viscoelastic layer. Moreover, two kinds of crossed ply specimens with stacking sequences labeled $[0_2/90_2]_s$, $[45_2/-45_2]_s$, and $[0_2/90_2/V]_s$, $[45_2/-45_2/V]_s$ were manufactured without and with a natural viscoelastic layer respectively as shown in Table 3. These specimens were chosen to favor damage mechanisms in particular configurations. $[90]_8$ specimens were assumed to favor matrix cracking and fiber-matrix interface failure. $[45]_8$ specimens were assumed to show a higher incidence of fiber-matrix debonding, due to a shear loading configuration. Fiber cracks were assumed to be detected just before the failure of specimens $[0]_8$. Due to interlaminar shear stress, delamination was expected to occur for $[0_2/90_2]_s$ and $[45_2/-45_2]_s$ specimens. Then, damage occurs by

debonding between the viscoelastic layer and stiff layers of the skin of viscoelastic laminate.

For the flexural tests, two types of unidirectional specimens were prepared, with fiber directions of 0° , with and without a natural viscoelastic layer. They were labeled $[0]_{16}$ and $[0_8/V]_s$ in Table 3.

Experimental setup

Experimental tests were carried out on a standard hydraulic machine INSTRON 8801. The capacity of the machine was ± 100 kN, capable of performing static and fatigue tests. The machine was interfaced with a dedicated computer for controlling and data acquisition as shown in Figure 1(a) and (b). The uniaxially loaded tensile tests were conducted using five rectangular specimens (see Table 3) of each type of composite (laminate and viscoelastic laminate) were in accordance with the standard test method ASTM D3039/D3039M.³² The strains in the tensile direction were measured by means of an extensometer with a gauge length of 25 mm as shown in Figure 1(a). The strains in the transverse direction were measured with 5 mm strain gauges. The tests were performed at room temperature with a displacement rate of 1 mm/min.

Table 2. The material properties of unidirectional flax/epoxy laminate.

	E_L (GPa)	E_T (GPa)	ν_{LT}	G_{LT} (GPa)	ρ (kg/m ³)
Flax fiber composite	22.2	3.23	0.4	1.33	1.15

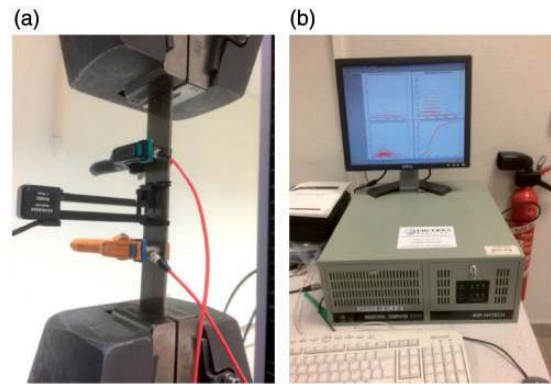


Figure 1. Experimental set up.

Table 3. Labeling of the materials and stacking sequence.

Tensile tests	$[90]_8$ $250 \times 25 \times 4$ mm ³	$[45]_8$	$[0]_8$	$[0_2/90_2]_s$	$[45_2/-45_2]_s$
Label	$[90_4/V]_s$ $250 \times 25 \times 5$ mm ³	$[45_4/V]_s$	$[0_4/V]_s$	$[0_2/90_2/V]_s$	$[45_2/-45_2/V]_s$
Flexural tests	$[0]_{16}$ $200 \times 15 \times 8$ mm ³ Span length 130 mm				
Label	$[0_8/V]_s$ $200 \times 15 \times 9$ mm ³ Span length 150 mm				

In the flexural test, rectangular specimens as shown in Table 3 of each type of composite (laminated and viscoelastic laminated) were tested in three-point bending in accordance with the ASTM D790-86 standard, at a span length of 130 mm for laminates and 150 mm for viscoelastic laminates. In static tests, the specimens were loaded at a constant rate of 2 mm/min. The fatigue tests were performed using sinusoidal type of waveform as a displacement control with a frequency of 5 Hz. Four mean displacements d_{mean} were maintained as constants equal to 15%, 40%, 50%, and 70% of displacement at failure in static tests, and amplitude of 1 mm was imposed. Three to five specimens were tested statically to failure and three to four specimens were tested in fatigue to failure for each of the two types of composites (laminated and viscoelastic laminated).

Two sensors with a bandwidth of 100 kHz–1 MHz, provided by Euro Physical Acoustics were clamped to the specimens (Figure 1(a)). A coupling agent was used between the sensors and the material. AE signals were registered with a sampling frequency of 5 MHz. Two preamplifiers with a 40 dB gain were used to amplify the signals. Pencil lead break tests were performed before each tensile test, to verify that the system was functioning properly, and to define an amplitude acquisition threshold (fixed at 40 dB) to filter acoustic signals coming from the test machine or other external sources. Only events recorded in the gauge length delimited by the two sensors were recorded. For each category of specimens broken in tension, macroscopic and microscopic analyses of the failure modes and mechanisms were performed. The failure profiles of the specimens were analyzed by scanning electron microscopy (SEM), in order to detect smaller damage mechanisms. In addition, microscopic sections were prepared with pieces of material extracted from untested and tested specimens.

Results

Tensile results

Figure 2 presents a comparative study of composite laminates with and without an embedded viscoelastic layer for unidirectional and cross-ply laminates. This figure presents typical stress/strain curves obtained by static monotonic tensile tests performed for each type of specimen. In Figure 2(a), specimens $[0]_8$ and $[0_2/90_2]_s$ made up of fibers aligned in the tensile direction, exhibit a short linear elastic domain followed by a nonlinear part, as observed by Monti et al.¹⁹ This behavior was not observed for traditional composites. The initial yield point, occurring for a very low deformation level and resulting in a significant loss of stiffness is visible on the stress/strain curves occurring at a strain level of 0.10%. This is a consequence of the nonlinear

behavior of the flax fibers themselves. This behavior is revealed by several mechanical analyses performed on single flax fibers, and is attributed to the yielding and viscous behavior of the lignin and amorphous cellulose of the fiber because of shear stresses in the cell walls.³³

After this yield point corresponding to a stress level of approximately 20 MPa, the static stress/strain curve appears to be quasi linear until failure which is of brittle type.

The stress–strain curves of the specimens $[45]_8$, $[90]_8$, and $[45_2/-45_2]_s$ show a nonlinear behavior up to rupture which is of the ductile type. This phenomenon is the consequence of the viscoelastic behavior of the resin. In the case of flax fiber reinforced composites with an interleaved natural viscoelastic layer, the stress/strain curves obtained by static monotonic tensile tests performed for every kind of specimen are shown in Figure 2(b). This figure shows that different mechanical characteristics such as rigidity, strength, and displacement at break of the viscoelastic laminate are lower than the values obtained in the case of the elastic ones. The two unidirectional composites $[0]_8$ and $[0_4/V]_s$ are stressed in the direction of the fibers, so they have higher elastic and breaking characteristics than the others. However, composites $[90]_8$ and $[90_4/V]_s$ have the weakest characteristics where only the resin is stressed in the tensile direction. In this case, the fibers do not contribute much to the behavior of the material. So that, the difference between each laminate configuration and its viscoelastic laminates counterpart decreases with the increase of the fiber orientation. The maximum is obtained between $[0]_8$ and $[0_4/V]_s$ specimens.

In order to highlight the damage mechanisms that appear during tensile tests, the various tests described previously were repeated, and the evaluation of the damage was carried out by AE. The AE data was processed with NOESIS software.³⁴ Five temporal parameters of the acoustic signals were selected for the classification of the data sets: amplitude, rise time, duration, absolute energy, and number of counts to peak. After multiple initial trials, these parameters have shown good repeatability of data clustering. They are illustrated in Figure 3. The K-mean algorithm³⁵ was used for the unsupervised pattern recognition. This algorithm aimed to separate a set of n events into an optimal number of k clusters in which each event belonged to the cluster with the nearest mean.

The application of the classification methodology returned the following results. Three classes were obtained for specimens $[90]_8$, $[45]_8$, and $[45_2/-45_2]_s$, whereas four classes were observed for specimens $[0]_8$ and $[0_2/90_2]_s$. Figure 4(a) presents the amplitudes of these AE classes with respect to the time and the applied load. Amplitude seems to properly separate

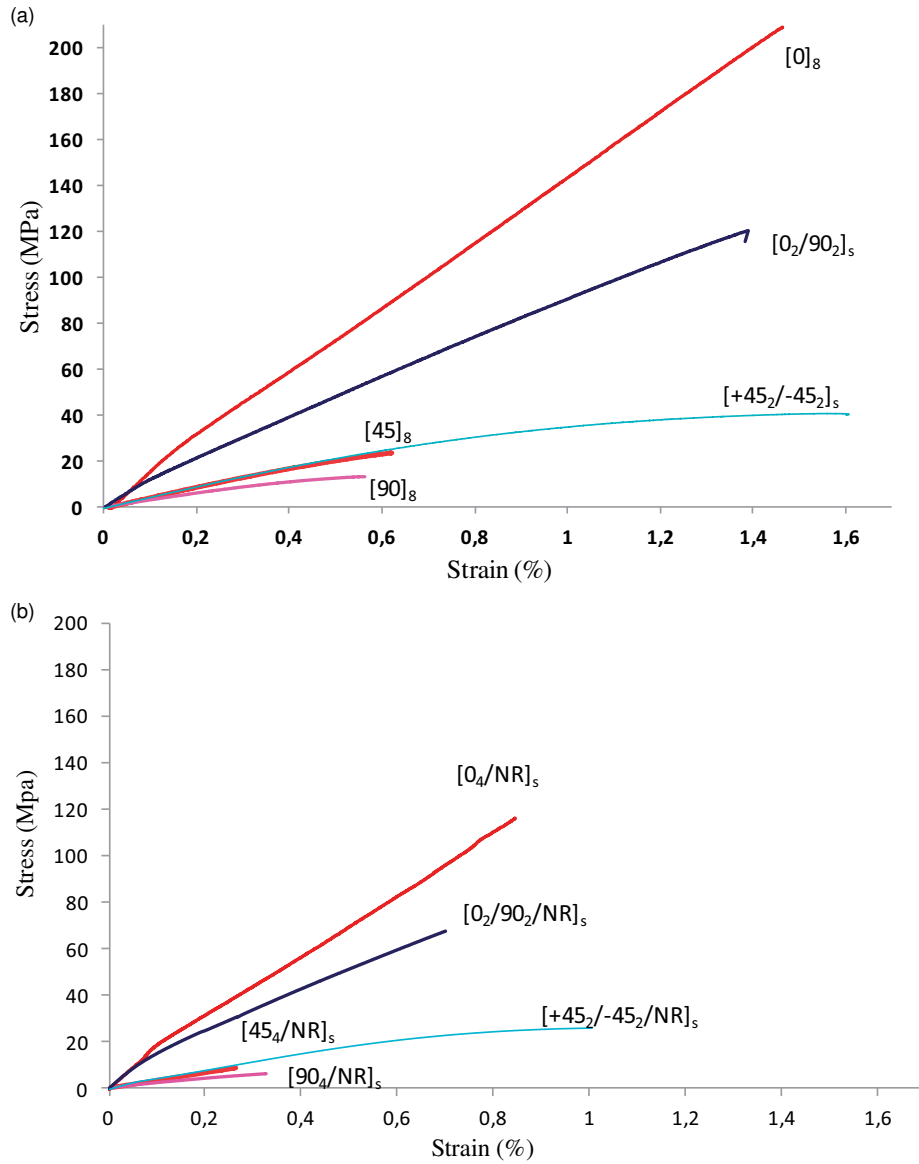


Figure 2. Stress/strain curves obtained by static monotonic tensile tests performed for flax fibers composites: (a) without viscoelastic layer and (b) with viscoelastic layer.

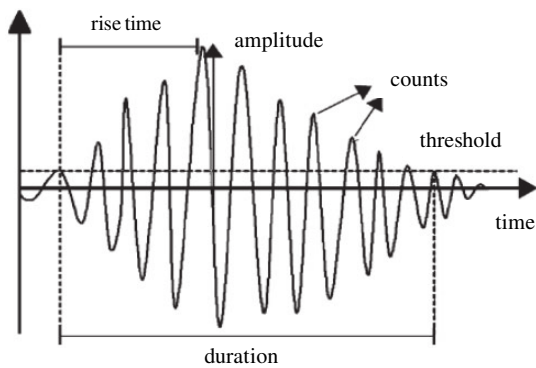


Figure 3. Typical waveform and parameters calculated by the acquisition system for each acoustic emission event.

these classes for specimens $[90]_8$, $[45]_8$, and $[45_2/-45_2]_s$. However, for the two other composites $[0]_8$, and $[0_2/90_2]_s$, involving a larger number of events, the very small areas of intersection between the different classes in the amplitude/time domain confirms that the choice of a multiparameter approach was appropriate and was confirmed by a principal component analysis (PCA) as shown in Figure 4(b). Figure 4(c) presents the cumulative number of hits for each class with respect to time. This is a good indication of the chronology and evolution of the acoustic events. For specimens $[90]_8$, $[45]_8$, and $[45_2/-45_2]_s$, the number of hits in classes A, B, and C increases progressively until the failure of the specimen. However, it presents a significant increase for specimens $[0]_8$, and $[0_2/90_2]_s$.

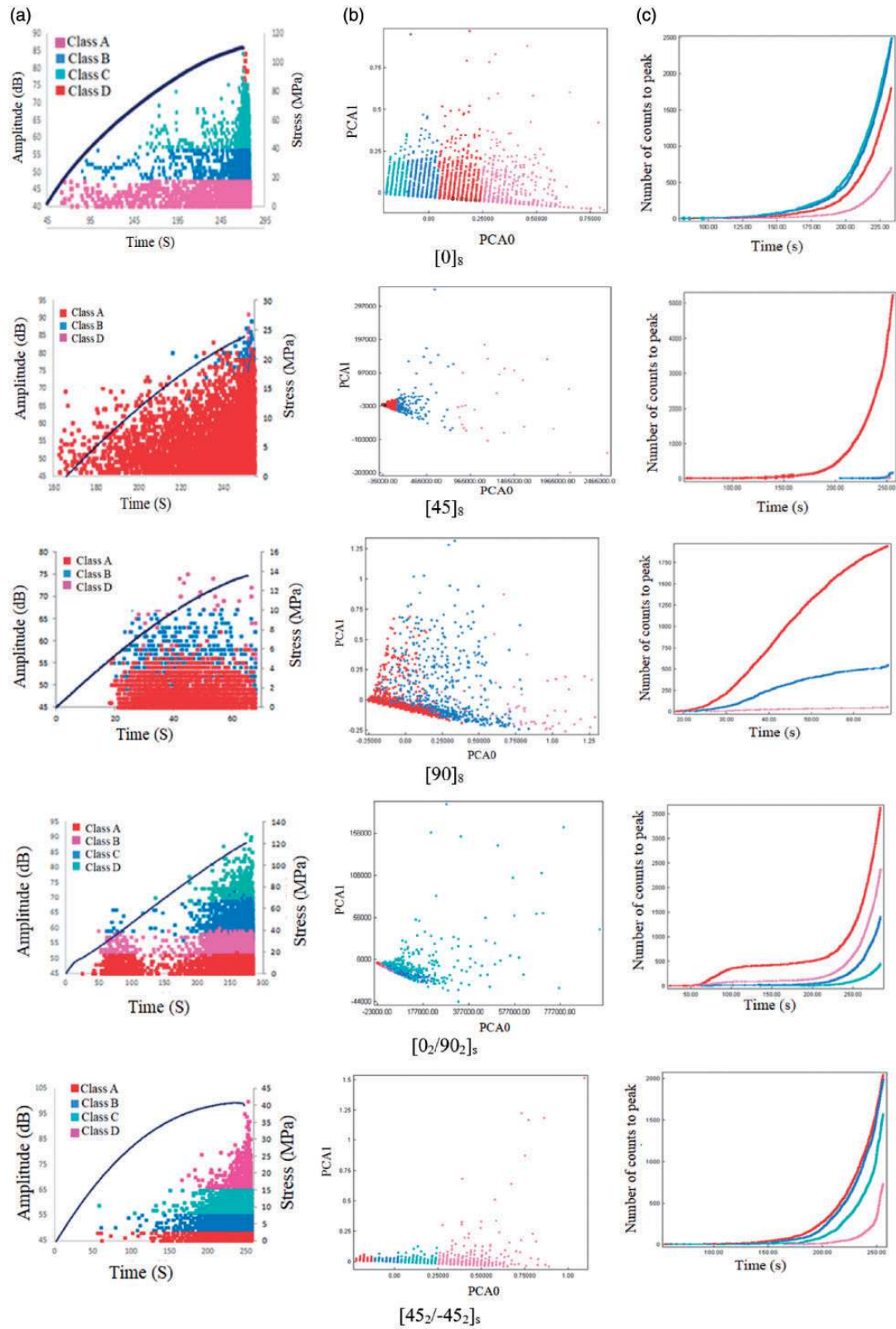


Figure 4. AE classification and analysis results for composite without viscoelastic layer: (a) Amplitude of the events and stress vs. time, (b) PCA axis, and (c) chronology of apparition of different classes.

In the case of composites with an interleaved natural viscoelastic layer, the application of the classification methodology yielded the following results as shown in Figure 5. Four classes were obtained for specimens $[90_4/V]_s$, $[45_4/V]_s$, and $[45_2/-45_2/V]_s$, whereas five classes were observed for specimens $[0_4/V]_s$, and $[0_2/90_2/V]_s$. An additional class appeared for those laminates compared to composites without an interleaved viscoelastic layer.

The AE classes shown previously were obtained by an unsupervised pattern recognition algorithm, which means that they constitute the best separation of the data regarding mathematical considerations, without really taking physics into account. Damage in natural fiber composites and its accumulation depend on many factors such as fiber volume fraction, fiber–matrix interface, stacking sequence, and applied stress level. In this perspective, failure profiles and micrographs have been observed by scanning electronic microscopes and are shown in Figure 6. This analysis was carried out in order to identify the acoustic signals emitted by different types of damages, also to compare these various mechanisms in materials with and without a viscoelastic layer during tests. Different damage mechanisms were identified on flax fiber/matrix composites from their AE signals.¹⁹ According to those previous studies and in order to associate each class obtained from the output of the classification algorithm with the damage mechanisms, the form characteristics of each class were considered.

The damage mechanisms considered according to the collected AE signals and SEM observation as shown in Figure 6 are matrix cracking “class A” (label 1), fiber/matrix debonding “class B” (label 2), delamination “class C” (label 3), fibers breaking “class D” (label 4), and interfacial composite/viscoelastic layer debonding “class E” (label 5). Typical waveforms of the five damage mechanisms collected are given in Table 4.

The acoustic signature of matrix cracking (class A) signal is characterized by slow rise time, low amplitude, and low energy. For fiber/matrix debonding (class B) signals, the waveform is characterized by a shorter rise time, higher amplitude, and higher energy. The acoustic signature of delamination (class C) is characterized by a very long duration, slow rise time, and higher energy. Signals for fibers breaking (class D) have a very short time, quick rise duration, high amplitude, and high energy. Finally, for interfacial debonding (class E) signals, the waveforms are characterized by very long duration, slow rise time, higher amplitude, and higher energy.

Flexural results

The effect of a viscoelastic layer on the transient response of a plate in static and fatigue flexural

responses was evaluated. Monotonic three point bending tests were conducted at a constant rate of 2 mm/min and carried out according the standard ASTM D790-86. Strength was measured by a load cell. Displacement was measured by a linear variable differential transformer (LVDT). Typical stress/strain curves derived from tests for laminate and viscoelastic laminated are presented in Figure 7. Flax fiber laminates and viscoelastic laminates show linear and nonlinear behavior until specimen failure. This evaluation proceeded in various stages: at the beginning of the test, the stress increased linearly with strain, and then the behavior became nonlinear up to maximum loading where it decreased nonlinearly for a short period before gradually decreasing until the rupture of the specimen. This phenomenon is a consequence of the nonlinear behavior of the flax fibers themselves and the natural viscoelastic layer. The behavior of flax fiber is revealed by several mechanical analyses performed on single flax fibers, and is attributed to the yielding and viscous behavior of the lignin and amorphous cellulose of the fiber because of shear stresses in the cell walls.¹⁹

In addition, it was observed that the stiffness and maximum stress of viscoelastic laminated were lower than the values obtained in the case of laminates without a viscoelastic layer. The flexural characteristics of the laminates and viscoelastic laminates from the static tests are reported in Table 5.

As in the case of the tensile tests, the application of the AE classification methodology in flexural tests returned the following results. Three classes were obtained for specimens $[0_{16}]_s$, whereas four classes were observed for specimens $[0_8/V]_s$. Figure 8(a) presents the amplitudes of these AE classes with respect to the time, superposed and the applied load. Amplitude seems to properly separate these classes for specimens $[0_{16}]_s$ and $[0_8/V]_s$. Figure 8(b) and (c) presents PCA and the cumulative number of hits for each class with respect to time. This is a good indication of the chronology and evolution of the acoustic events. For all test specimens, the number of hits in classes A, B, and C increase progressively until the failure of the specimen. As in tension, viscoelastic laminates have an additional class.

Fatigue tests were performed on cross flax fiber laminates and viscoelastic laminates using sinusoidal type of waveform at a loading of frequency of 5 Hz. The applied mean displacement level (50% of failure displacement) was chosen in order to cover the significant active regions (damage development) of stress/strain curve as shown in Figure 7, at a fixed displacement amplitude of 1 mm. Dynamic flexural fatigue tests were performed using cylindrical rollers having a 20 mm diameter. The tests were conducted at room temperature under displacement control.

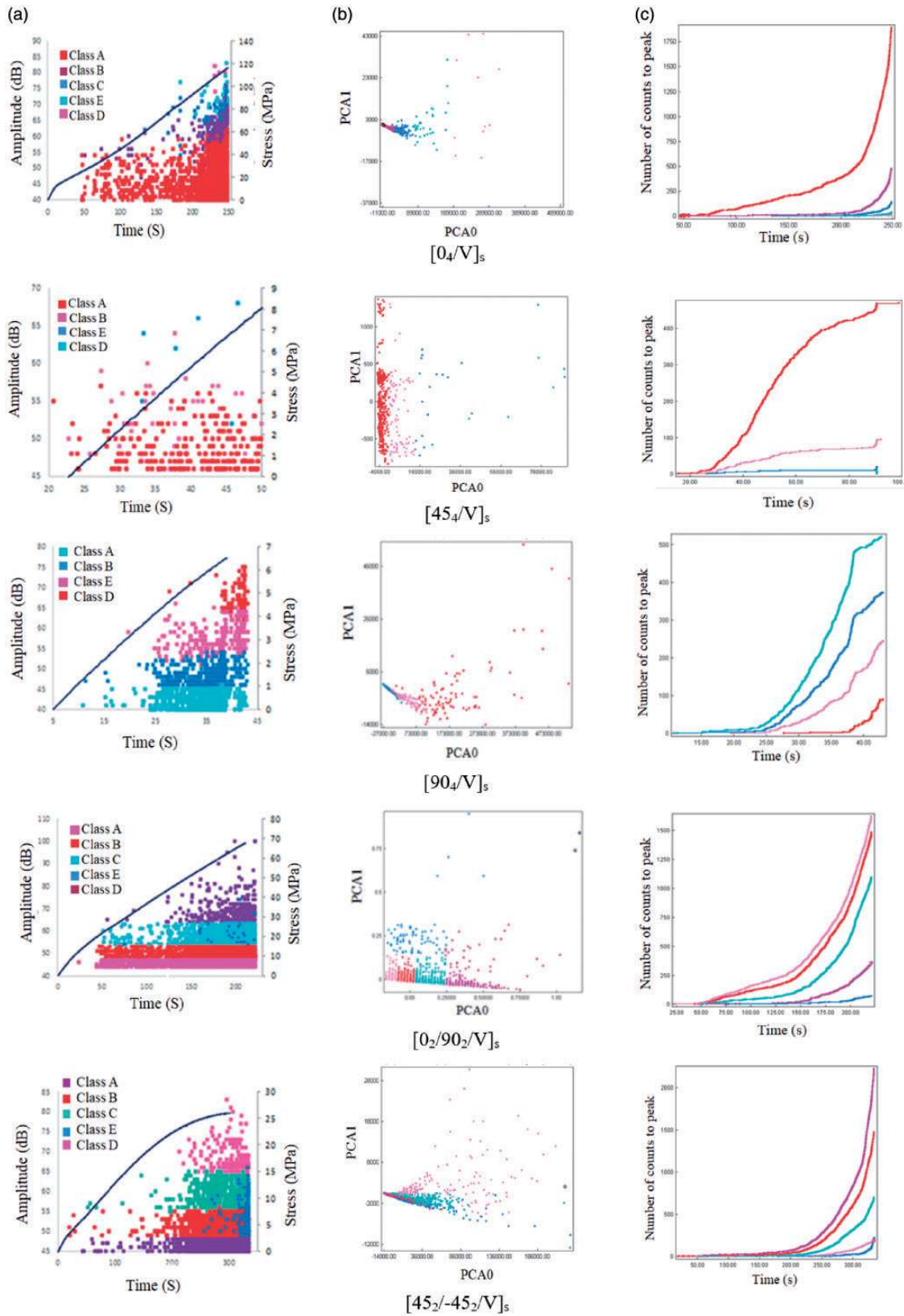


Figure 5. AE classification and analysis results for composite with viscoelastic layer: (a) Amplitude of the events and stress vs. time, (b) PCA axis, and (c) chronology of apparition of different classes.

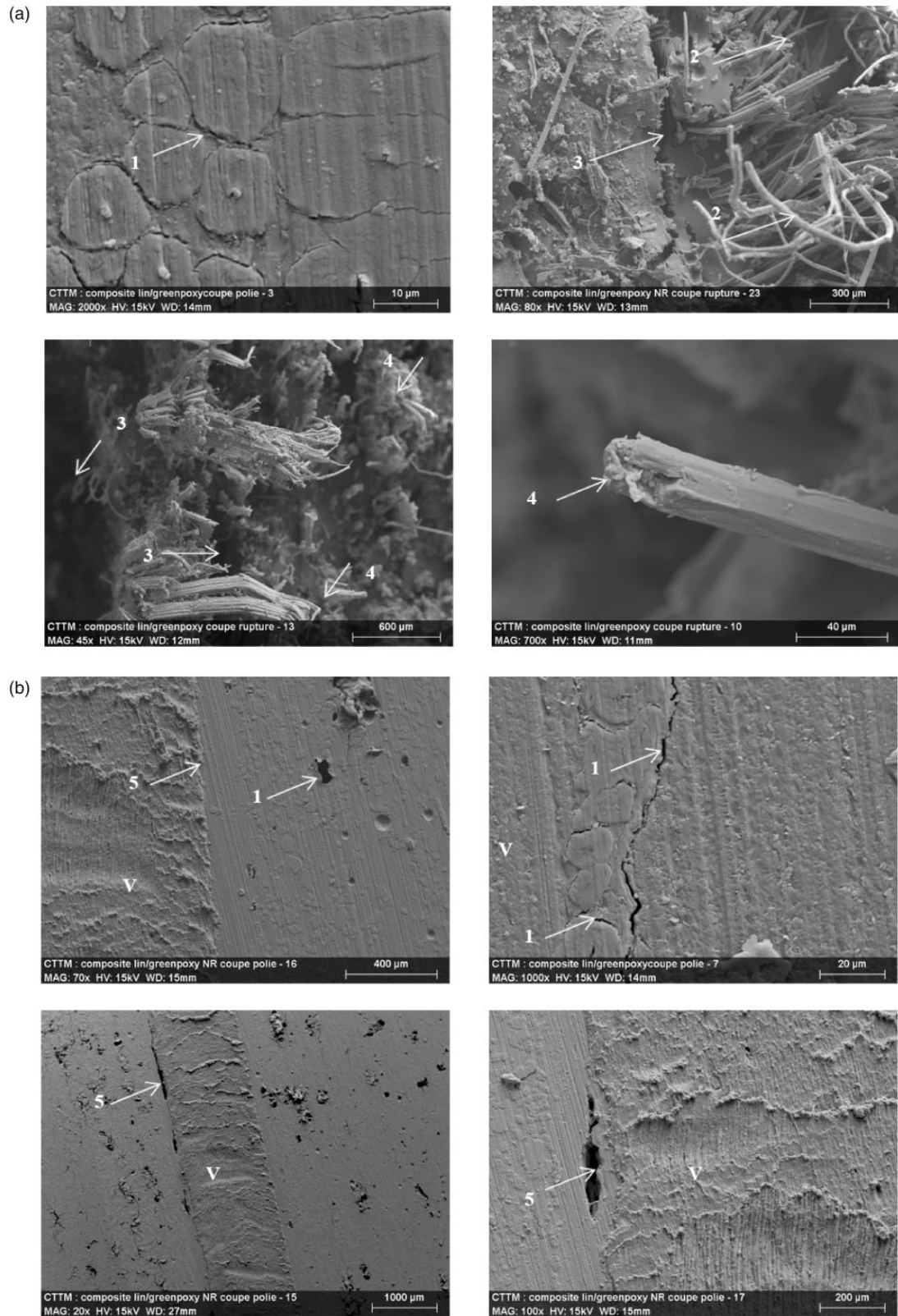
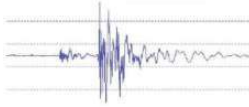

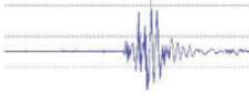
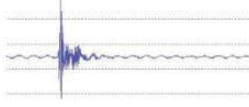



Figure 6. SEM observations of failure profiles and micrographs of flax fiber composites: (a) without viscoelastic layer and (b) with viscoelastic layer (V).

Table 4. Typical waveforms of the five damage mechanisms.

Class A	Matrix cracking	
Class B	Fiber/matrix debonding	
Class C	Delamination	
Class D	Fiber breaking	
Class E	Interfacial composite/viscoelastic layer debonding	

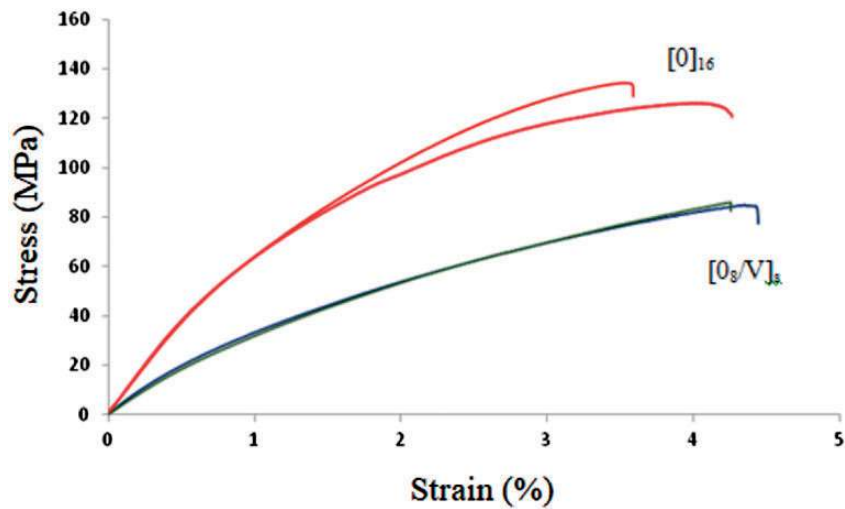


Figure 7. Typical stress/strain curves derived from three point bending tests.

Table 5. Flexural characteristics of the laminate and viscoelastic laminate.

	Young's modulus (MPa)	Failure stress (MPa)	Failure strain (%)
Laminate	15.4	135	3.9
Viscoelastic laminate	9.8	75	4.5

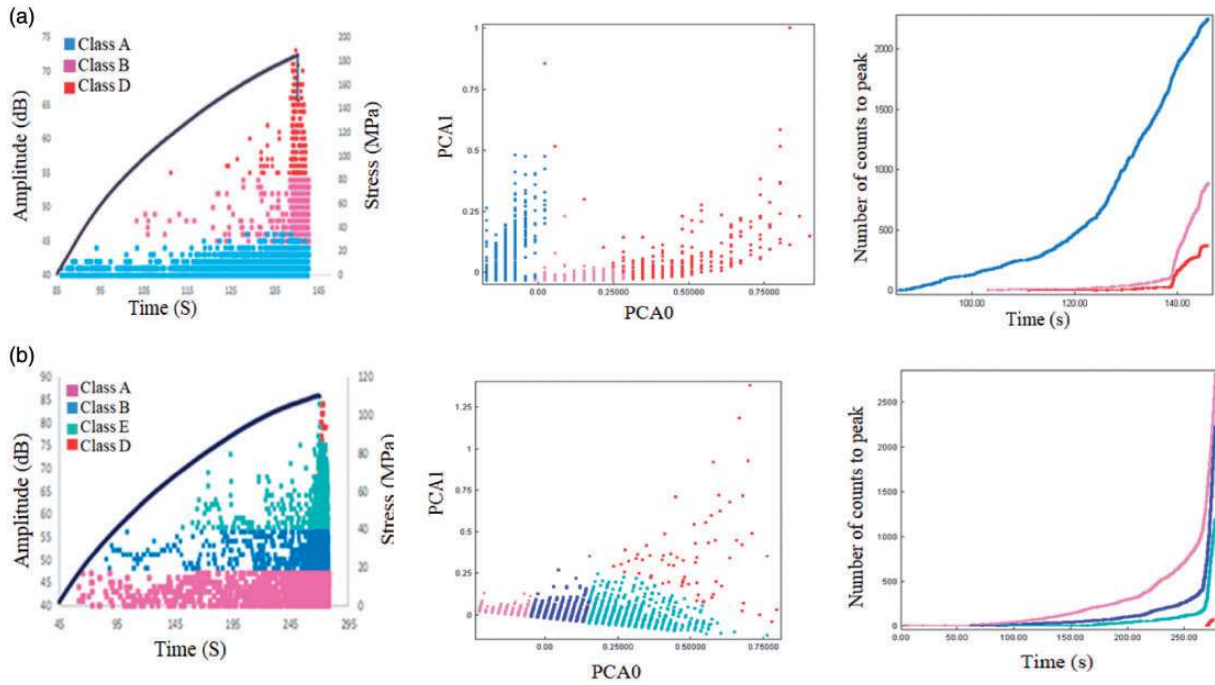


Figure 8. AE classification and analysis results in flexural static tests for composite (a) without viscoelastic layer $[0]_{16}$ and (b) with viscoelastic layer $[0_8/V]_s$.

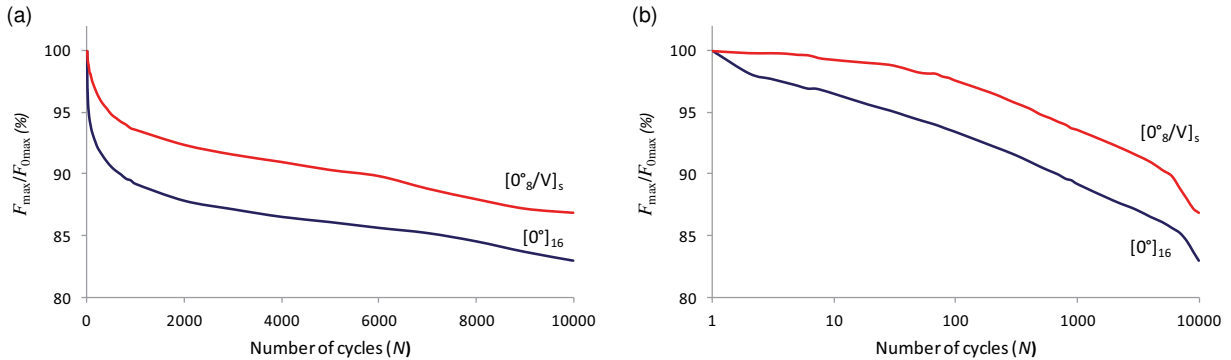


Figure 9. Variation of the maximum applied load as a function of cycle number in flexural fatigue tests for composite with $[0_8/V]_s$ and without $[0]_{16}$ viscoelastic layer: (a) linear scale and (b) logarithmic scale.

During fatigue with displacement control, it was almost universal that load decreases as cycling continues, causing stiffness to decrease. Hysteresis curves, energy dissipation curves, and stiffness versus number of cycles' diagrams were generated, and the failure mechanisms were examined. Figure 9 shows a typical result of a fatigue test, which present the evolution of the maximum load as a function of the number of cycles using a linear (Figure 9(a)) and semilogarithmic scale (Figure 9(b)). The maximum load F_{max} was compared to that obtained in the first cycle F_{0max} . The results of the composite with and without a viscoelastic layer are presented in the same figure for comparison.

For a given composite, the loss of rigidity, which was presented by the load ratio F_{max}/F_{0max} , was presented in two phases: the first one showed a significant decrease in the first cycles, which could be associated with the initiation and multiplication of cracking in the resin and the fibers. This decrease was about 7% for the composite with a viscoelastic layer and 12% for the composite without the natural rubber. Then, the stiffness decreases very slowly and quasi-linearly corresponding to progressive evolution of the damage mechanisms. This behavior is commonly observed for composite structures. It is worth noticing that the $[0]_{16}$ without viscoelastic layer present a higher degradation

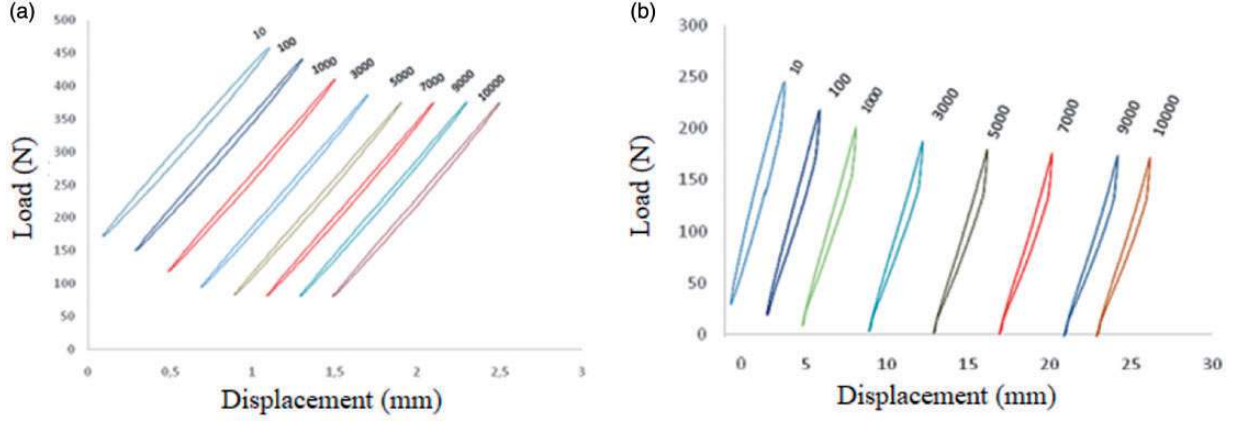


Figure 10. Hysteresis curves as a function of cycle number in flexural fatigue tests for composite: (a) without viscoelastic layer $[0_{16}]$ and (b) with viscoelastic layer $[0_8/V]_s$.

rate and fail earlier than composite with viscoelastic layer $[0_8/V]_s$. The use of the fixed displacement level for both materials, leads two different stress levels of composites. Indeed, the viscoelastic composite is loaded in a stress range between 35 MPa and 70 MPa, while the elastic composite is loaded in a range from 65 MPa to 125 MPa. This indicates that the elastic composite is more damaged under flexural loading than the viscoelastic composite (Figure 9).

The different hysteresis loops were then obtained from the experimental load and displacement data. Figure 10 presents the evolution of the hysteresis obtained with the number of cycles at 10, 100, 1000, 3000, 5000, 7000, 9000 and 10,000 cycles. The curves have been shifted along the displacement axis in order to clarify the figure. It can be seen that hysteresis loops in the first cycle have large area in loading and unloading and high peak load for two composite materials. With the increase of the number of cycles area under the hysteresis loops and peak of the load decreases due to the damage development in the constituents of composites. With the increasing number of cycles, there is a deviation of the hysteresis curve. The deviation becomes important at 10^4 cycles for the composite with a viscoelastic layer. This deviation in the hysteresis loop shows that the dynamic response of the composite with the natural rubber on loading is different from the response on unloading.

The areas for the hysteresis loops present the dissipated energy E_d and the areas under the upper part of the curves represent the potential energy E_p . These quantities (E_d and E_p) have been calculated numerically using the trapezoid method. Figure 11(a) shows the dissipated energy E_d as a function of the number of cycles for the composites with and without a viscoelastic layer. For the two different composites, the dissipated energy decreases as the number of cycles increases. This decrease take place in two phases: the

first one is large decrease in the first cycles followed by the second one, which is characterized by a very slow decrease (stabilization). It is also clear that the insertion of the viscoelastic layer in the composites significant increase the values of the dissipated energy. The dissipated energy is about two times higher in the composite with a viscoelastic laminate than in the composite without a viscoelastic layer.

The loss factor of the composite could be influenced by different parameters such as the fiber/matrix interface, the damage, the porosities, and the viscoelastic behavior of the different components making up the structure. The loss factor η was calculated in the cyclic fatigue tests as follows

$$n = \frac{E_d}{2\pi E_p} \quad (1)$$

where E_d is the dissipated energy and E_p is the maximum potential energy.

Figure 11(b) shows the variation in the loss factor as a function of the number of cycles for the composite with and without the viscoelastic layer. The curves present a decrease of this factor in the first cycles, and it becomes almost constant after a few hundred cycles. Moreover, the composite with a viscoelastic layer presents very high values, which vary between 2 and 4 times higher in the composite with viscoelastic compared with those without a viscoelastic layer. Therefore, this viscoelastic layer significantly improves the damping behavior of the structure. As in the case of the static tests, an AE analysis of the damage was carried out. The classification of the different damage modes in the fatigue tests were done on unidirectional specimens with and without viscoelastic layer $[0_{16}]$ and $[0_8/V]_s$. Figure 12 presents the classification results of AE data. The acoustic activity during the fatigue tests was divided into three phases (Figure 12(a)) for

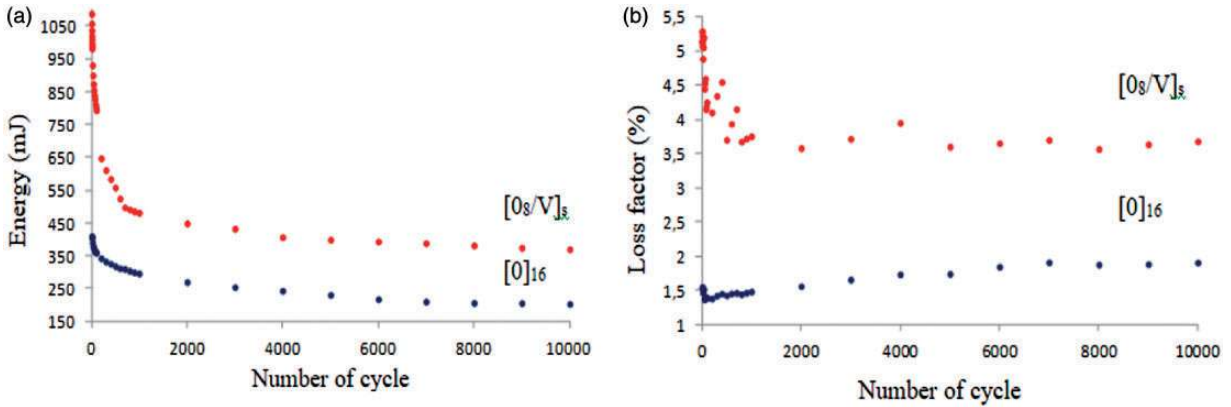


Figure 11. Dissipated parameters as energy as a function of the number of cycles with and without viscoelastic layer: (a) dissipated energy and (b) loss factor.

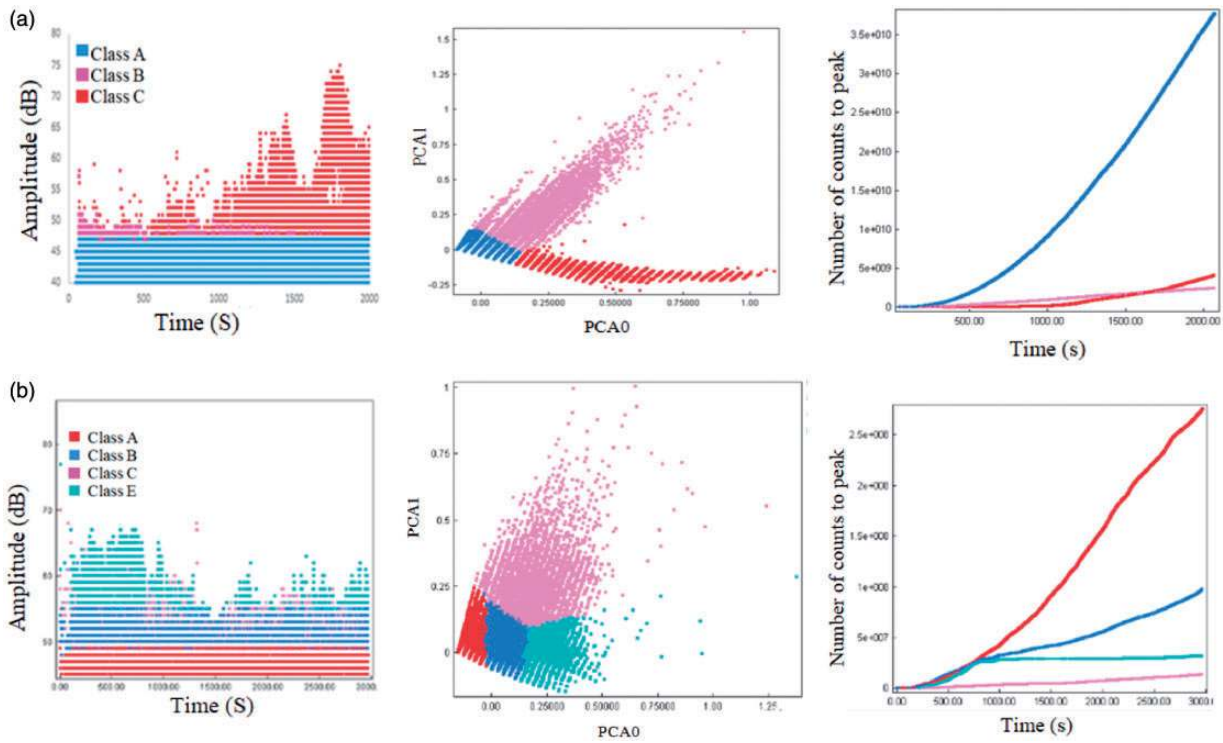


Figure 12. AE classification and analysis results in flexural fatigue tests for composite (a) without viscoelastic layer $[0]_{16}$ and (b) with viscoelastic layer $[0_8/V]_s$.

specimen $[0]_{16}$, and four phases (Figure 12(b)) for specimen $[0_8/V]_s$. In this case also, an additional class was observed on the viscoelastic laminates.

For the laminate without a viscoelastic layer, there was little overlap of the amplitudes of the different classes. These classes may be associated with damage mechanisms based on the results and the analysis performed in static tests. This discrimination of the damage mechanisms can thus be justified from results

in such as those of Bravo et al.,²⁸ and Aslan.²⁹ These results were carried out on the acoustic characteristics of the main damage mechanisms for natural flax fiber composites. Thus, the damage mechanisms considered according to the collected AE signals are as follows: “class A” matrix cracking, “class B” fiber/matrix debonding, and “class C” delamination.

For viscoelastic laminates, the mechanism of debonding between the composite and the viscoelastic

layer was also observed. Small areas of overlap between amplitudes have been observed. The identification of the different damage mechanisms led to the following results: “Class A” matrix cracking, “class B,” fiber/matrix debonding, “class C” delamination and “class E” composite/viscoelastic layer debonding

Conclusion

The mechanical behavior in static and fatigue tests of the flax fiber composites with and without an interleaved natural viscoelastic layer was studied. Uniaxial static loading tests were performed on specimens having different stacking sequences. Moreover, three-point bending tests in static and cyclic fatigue tests were performed on unidirectional specimens in the 0° direction. The various tests were followed by AE analysis to identify and evaluate the different damage mechanisms. Microscopic analyses, associated with this approach, made it possible to identify the various damage mechanisms during the tests. The results obtained show three or four classes of damage (matrix cracking, fiber/matrix debonding, delamination, and fiber breakage) according to the stacking sequence for elastic laminates and four or five classes for viscoelastic laminates. An additional class “debonding composite/viscoelastic layer” was obtained in the case of viscoelastic laminates for all static and cyclic fatigue tests.

The laminates studied can be used as a substitution or supplement for applications using conventional composites reinforced with synthetic fibers. They can also be used in the design of materials for improving the dynamic response of structures by a high level of energy dissipation.


Declaration of Conflicting Interests

The author(s) declared no potential conflicts of interest with respect to the research, authorship, and/or publication of this article.

Funding

The author(s) received no financial support for the research, authorship, and/or publication of this article.

ORCID iD

Hajer Daoud  <http://orcid.org/0000-0001-6031-5790>

References

1. Yan L, Chou N and Jayaraman K. Flax fiber and its composites—a review. *Compos Part B* 2014; 56: 296–317.
2. Wambua P, Ivens J and Verpoest I. Natural fibers: can they replace glass in fiber reinforced plastics? *Compos Sci Technol* 2003; 63: 1259–1264.

3. Libo Y, Nawawi C and Krishnan J. Flax fiber and its composites—a review. *Compos Part B Eng* 2014; 56: 296–317.
4. Monti A, El Mahi A, Jendli Z, et al. Experimental and finite elements analysis of the vibration behavior of a bio-based composite sandwich beam. *Compos Part B Eng* 2017; 110: 466–475.
5. Poilâne C, Cherif ZE, Richard F, et al. Polymer reinforced by flax fibers as a viscoelastoplastic material. *Compos Struct* 2014; 12: 100–112.
6. Placet V. Characterization of the thermo mechanical behaviour of Hemp fibers intended for the manufacturing of high performance composites. *Compos Part A* 2009; 40: 1111–1118.
7. Yan Li, Yiu-wing Mai and Lin Ye. Sisal fiber and its composites: a review of recent developments. *Compos Sci Technol* 2006; 60: 2037–2055.
8. Assarar M, El Mahi A and Berthelot J-M. Damping analysis of sandwich composite materials. *J Compos Mater* 2009; 43: 1461–1485.
9. Bhimaraddi A. Sandwich beams theory and the analysis of constrained layer damping. *J Sound Vibrat* 1995; 179: 591–602.
10. Khalfi B and Ross A. Transient response of a plate with partial constrained viscoelastic layer damping. *Int J Mech Sci* 2013; 68: 304–312.
11. Saravanos DA and Pereira JM. Effects of interply damping layers on the dynamic characteristics of composite plates. *AIAA J* 1992; 30: 2906–2913.
12. Cupial P and Niziol J. Vibration and damping analysis of a three-layered composite plate with a viscoelastic mid-layer. *J Sound Vibrat* 1995; 183: 99–114.
13. Yim JH, Cho SY, Seo YJ, et al. A study on material damping of 0 laminated composite sandwich cantilever beams with a viscoelastic layer. *Compos Struct* 2003; 60: 367–374.
14. Ni RG and Adams RD. The damping and dynamic moduli of symmetric laminated composite beams. Theoretical and experimental result. *Compos Sci Technol* 1984; 18: 104–121.
15. Monti A. *Elaboration et caractérisation mécanique d'une structure sandwich à base de constituant naturels*. PhD Thesis, Le Mans University, Le Mans, France, 2017.
16. Masmoudi S, El Mahi A and Turki S. Fatigue behaviour and structural health monitoring by acoustic emission of E-glass/epoxy laminates with piezoelectric implant. *Appl Acoust* 2016; 108: 50–58.
17. Huguet S. *Application de classificateurs aux données d'émission acoustique: identification de la signature acoustique des mécanismes d'endommagement dans les composites à matrice polymère*. PhD Thesis, INSA, Lyon, France, 2002.
18. Bourchak M, Farrow IR, Bond IP, et al. Acoustic emission energy as a fatigue damage parameter for CFRP composites. *Int J Fatigue* 2007; 29: 457–470.
19. Monti A, El Mahi A, Jendli Z, et al. Mechanical behaviour and damage mechanisms analysis of a flax-fiber reinforced composite by acoustic emission. *Compos Part A* 2016; 90: 100–110.

20. Li L, Lomov SV and Yan X. Correlation of acoustic emission with optically observed damage in a glass epoxy woven laminate under tensile loading. *Compos Struct* 2015; 123: 45–53.
21. Gutkin R, Green CJ, Vangrattanachai S, et al. On acoustic emission for failure investigation in CFRP: pattern recognition and peak frequency analyses. *Mech Syst Signal Process* 2011; 25: 1393–1407.
22. de Groot PJ, Wijnen PAM and Janssen RBF. Real-time frequency determination of acoustic emission for different fracture mechanisms in carbon epoxy composites. *Compos Sci Technol* 1995; 55: 405–412.
23. Sause MGR, Gribov A, Unwin AR, et al. Pattern recognition approach to identify natural clusters of acoustic emission signals. *Pattern Recognit Lett* 2012; 33: 17–23.
24. De Rosa IM, Santulli C and Sarasini F. Acoustic emission for monitoring the mechanical behaviour of natural fiber composites: a literature review. *Compos Part A Appl Sci Manuf* 2009; 40: 1456–1469.
25. El Mahi A, Ben Salem I, Assarar M, et al. Analyse par émission acoustique de l'endommagement des matériaux éco-composites. CFA2010 10ème Congrès Français d'Acoustique, 2010.
26. Elouaer A, Aboura Z, Ayad R, et al. Monitoring of fatigue damage in composites based fiber plant. *Journées Natl des Compos* 2009; 70–71.
27. Kersani M, Lomov SV, van Vuure AW, et al. Damage in flax epoxy quasi unidirectional woven laminates under quasi static tension. *J Compos Mater* 2015; 49: 403–413.
28. Bravo A, Toubal L, Koffi D, et al. Characterization of tensile damage for a short birch fiber-reinforced polyethylene composite with acoustic emission. *Int J Mater Sci* 2013; 3: 79–89.
29. Aslan M. Investigation of damage mechanism of flax fiber LPET commingled composites by acoustic emission. *Compos Part B Eng* 2013; 54: 289–297.
30. Saeedifar M, Fotouhi M, Ahmadi Najafabadi M, et al. Prediction of quasi-static delamination onset and growth in laminated composites by acoustic emission. *Compos Part B Eng* 2016; 85: 113–122.
31. Khalfallah M, Abbès B, Abbès F, et al. Innovative flax tapes reinforced Acrodur biocomposites: a new alternative for automotive applications. *Mater Des* 2014; 64: 116–126.
32. A. D30309/D3039M-14. Standard test method for tensile properties of polymer matrix composite.
33. Placet V, Cissé O and Lamine Boubakar M. Nonlinear tensile behaviour of elementary hemp fibers. Part I: investigation of the possible origins using repeated progressive loading with in situ microscopic observations. *Compos Part A Appl Sci Manuf* 2014; 56: 319–327.
34. NOESIS software. Advanced acoustic emission data analysis pattern recognition and neural networks software, 2004.
35. Likas A, Vlassis N and Verbeek J. The global k-means clustering algorithm. *Pattern Recognit* 2003; 36: 451–461.